COBEM 2023 27TH INTERNATIONAL CONGRESS OF MECHANICAL ENGENEERING

ABCM Brazilian Society of Mechanical Sciences and Engineering
27th ABCM International Congress of Mechanical Engineering
December 04-08, 2023, Florianópolis-SC, Brazil

COB-2023-0145
INVESTIGATION OF THE TOOL-CHIP INTERFACE TEMPERATURE IN CRYOGENIC TURNING OF HARDENED AISI D6 TOOL STEEL

Edmilson Dantas de Lima Júnior
Federal Institute of Education, Science and Technology of Rio Grande do Norte, 160 BR-101, S/N - Areia Branca, Canguaretama/RN, Brazil.
e-mail: edjr.013@gmail.com

Anderson Clayton Alves de Melo
Adilson José de Oliveira
Federal University of Rio Grande do Norte, Senador Salgado Filho Avenue, 3000 - Lagoa Nova, Natal/RN, Brazil.
e-mail: anderson.melo@ufrn.br, adilson.oliveira@ufrn.br

Júlio César Giubilei Milan
Santa Catarina State University, Paulo Malschitzki Street, 200 - Zona Industrial Norte, Joinville/SC, Brazil.
e-mail: julio.milan@udesc.br

Álisson Rocha Machado
Mechanical Engineering Graduate Program, Pontifícia Universidade Católica do Paraná – PUC-PR, Curitiba, PR, Brasil.
e-mail: alisson.rocha@pucpr.br

Abstract. *Hard turning is considered a strong candidate to partially replace grinding in finishing operations. However, it produces high temperatures that contributes to accelerate the cutting tool wear. To minimize this effect, mineral-based cutting fluids can be applied, although there are many drawbacks associated with the use of these cutting fluids as they are hazardous to the environment. In this context, the need for more eco-friendly cutting fluids is growing and liquid nitrogen (LN2) offers a promising alternative. Previous studies have shown that LN2 can significantly reduce the cutting tool wear in comparison with other cooling strategies, and this is normally attributed to a reduction in the tool-chip interface temperature. However, investigations on the tool-chip interface temperature in cryogenic machining are scarce in the literature, particularly regarding the turning of tool steels. Thus, in this study, the tool-chip interface temperature during the turning of quenched and tempered AISI D6 tool steel, under dry and using LN2, was investigated. A tool-workpiece thermocouple system was developed for this purpose and calibrated using a data acquisition system based on the Arduino Uno platform. In the turning tests, liquid nitrogen was delivered at the tool flank face of PCBN inserts at three cutting speeds with a constant feed rate and depth of cut. The results showed that LN2 was able to reduce the tool-chip interface temperature at the lowest cutting speed; however, when this cutting parameter was increased, the reduction in the interface temperature was minimal as compared with the dry condition.*

Keywords: *Hard turning, Tool-chip interface temperature, Hardened AISI D6 tool steel, Cryogenic machining.*

1. INTRODUCTION

Because of its relative low cost and flexibility, hard turning has been proposed to partially replace the grinding operation in the manufacturing of hardened steel parts with high accuracy and surface quality (Dosbaeva et al., 2015). According to Sharma et al. (2015), when compared with grinding, hard turning presents several advantages, such as reduced set-up and manufacturing times. Additionally, hard turning produces a machined surface with longer rolling contact fatigue life as compared to a ground surface, with the same or even lower average surface roughness (Hashimoto et al., 2006). Besides these technical advantages, hard turning is less environmentally harmful than grinding if the operation is performed under dry conditions. In this case, the process can be considered as eco-friendly, because there is no residue from cutting fluids, which are usually mineral-based emulsions that are extremely harmful to the environment and human health, besides being costly (Benedicto et al., 2017). In this context, there is increasing pressure from governmental and non-governmental entities for industries to adopt cleaner production technologies (Malek and Desai, 2019).

Although dry hard turning presents many advantages over grinding, it also leads to high cutting temperatures, which promote thermally-induced wear mechanisms at the cutting edge, such as diffusion and oxidation, leaving the tool more prone to adhesion and abrasion and reducing the cutting tool life (Del Re et al., 2019). Thus, in the search for improved methods of machining hardened steel components, the contemporary context of sustainability needs to be considered,

seeking solutions that address technical, economic, environmental and health issues. In this regard, an alternative that has been extensively investigated in recent years is LN2-assisted machining.

Several previous investigations have shown the many benefits of using LN2 as a cutting fluid in the turning of difficult-to-machine materials instead of dry or conventional flood machining. In most cases these benefits are presented in terms of increased cutting tool life, and consequently decreased tool wear rate, increased workpiece surface hardness and surface compressive residual stresses, and improved surface roughness (Leadebal Jr. et al., 2019a, 2019b; Shokrani et al., 2013; Biček et al., 2012).

Shokrani et al. (2013) published a comprehensive review of recent advances in the area of cryogenic machining and processing. They highlighted the effects of cryogenic cooling on the workpiece behavior during machining and on the machinability output parameters, such as tool life, cutting temperature and surface integrity, for various tool-workpiece pairs. With regard to hard-to-cut materials, such as hardened steels, they noted that high temperatures are generated in the cutting zone, affecting the tool life, surface finish and geometrical accuracy of the machined part. In this situation, cooling the cutting zone with a cryogenic fluid not only cools the cutting zone but can also change the workpiece and cutting tool material properties, which can improve the machining process performance. With regard to the tribological behavior of materials at cryogenic temperatures, Shokrani et al. (2013) reported that a cryogenic temperature is generally expected to change the tribological behavior of the sliding surfaces by increasing the surface hardness and reducing the interface temperature.

Biček et al. (2012) machined quenched and tempered AISI 52100 bearing steels bars, with hardness of 850 HV (~64 HRc) under cryogenic (with LN2) and dry conditions for comparison. They reported that, in contrast to dry cutting, LN2-assisted turning did not produce the fragile white layer beneath the workpiece surface, partially due to lower cutting temperatures provided by the liquid nitrogen.

Hong and Ding (2001) investigated the efficiency of five methods of cryogenic turning assisted by liquid nitrogen in the machining of Ti-6Al-4V alloy, i.e., delivering LN2 at the rake face, flank face, or at both faces close to the main cutting edge, precooling the workpiece, and cooling the bottom of the tool. For comparison, they also performed turning trials under dry conditions and applying a conventional flood emulsion. The cutting temperatures were theoretically estimated using the finite element method (FEM), considering heat transfer and two-dimensional numerical modeling approaches. These were experimentally validated using a K-type thermocouple embedded in a carbide insert. All numerical computational models considered a depth of cut of 1.27 mm, a feed rate of 0.254 mm/rev and cutting speeds of 60, 90, 120, and 150 m/min. It was concluded that applying LN2 on the rake and flank faces simultaneously provided the lowest temperature at the tool-chip interface, reducing it to less than 500 °C, even at the highest cutting speed.

Dhar et al. (2002) performed an investigation similar to that of Hong and Ding (2001). They studied the influence of LN2 on the tool-chip interface temperature when turning AISI 1040 plain carbon steel with two types of cemented carbide inserts (SNMG 120408-26 TTS and SNMM 120408 TTS, by WIDIA). Dry turning tests were also performed for comparison. As in the case of Hong and Ding (2001), they also used a two-dimensional finite element model to estimate the temperature distribution in the cutting tool, chip and workpiece. The experimental method used to obtain the tool-chip interface temperatures was the tool-workpiece thermocouple technique. Experiments were performed varying the feed rate (0.12, 0.16, 0.20 and 0.24 mm/rev) and the cutting speed (66, 85, 110 and 144 m/min), keeping the depth of cut constant and equal to 1.5 mm. On analyzing the distribution of temperatures obtained through the finite element model, it was noted that the maximum temperature occurred at around the middle of the tool-chip contact length regardless of the cutting strategy (dry or LN2), as also observed by Hong and Ding (2001) when turning Ti-6Al-4V alloy. It was also noted that the application of liquid nitrogen substantially reduced the maximum temperature at the tool-chip interface and the wear land for both inserts, besides making the chips curl more than under dry cutting, reducing the tool-chip contact length.

Based on reports published on the subject addressed herein, it can be noted that there is a consensus among researchers that LN2-assisted machining is able to reduce the cutting temperature, even at the tool-chip interface, increasing the cutting tool life and improving the surface integrity in many cases. However, studies involving the measurement of cutting temperatures during the cryogenic turning of hardened tool steels are scarce. Thus, aiming to contribute to fill this gap, in this study the tool-chip interface temperatures when turning quenched and tempered AISI D6 steel under dry and cryogenic condition were estimated using a tool-workpiece thermocouple system that was developed based on research by Kaminise et al. (2014), which will be described in the next section.

2. TOOL-WORKPIECE THERMOCOUPLE TECHNIQUE

According to Shaw (2005), the tool-workpiece thermocouple technique was developed almost simultaneously in the 1920s by Shore in the United States, Gottwein in Germany and Herbert in Great Britain. It is used to determine the average tool-chip interface temperature and is based on the fact that an electromotive force (EMF) is generated at the interface of two dissimilar metals when the temperature of the interface changes, as in the case of the contact between workpiece and cutting tool during turning procedures.

The laws of thermoelectric circuits applicable to the tool-workpiece thermocouple technique are (Shaw, 2005):

1. The EMF in a thermoelectric circuit is solely dependent on the difference between the temperatures of the hot and cold junctions and it is independent of the gradients in the parts making up the system.
2. The EMF generated is independent of the size and resistance of the conductors.
3. When the junction of two metals is at uniform temperature, the EMF generated is not affected if a third metal, which is at the same temperature, is used to make the junction between the first two.

In practice, the application of these principles in turning process can be explained by analyzing Figure 1(a). The tool-chip contact forms the hot junction "H", while the points "A" and "B" constitute the cold junctions, which remain at room temperature. Mercury is normally used to establish electrical contact with the rotating shaft, allowing the closing of the circuit. The connection wires "C" and "D" can be made of simple copper wires, which must be kept at the same temperature in order to prevent an unwanted signal. It is important to mention that the mercury can be placed inside a modified live center in the tailstock, as in this investigation. To transform the electrical signal into temperature, an appropriate method of calibration is needed. Shaw (2005) presented the arrangement shown in Figure 1(b) as the simplest and most accurate approach to calibration in the tool-workpiece thermocouple technique.

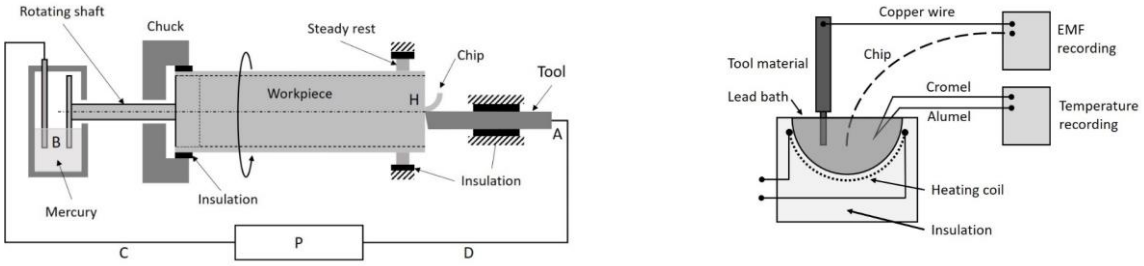

(a) (b)

Figure 1. (a) Tool-workpiece thermocouple technique; (b) Arrangement for calibration in the tool-workpiece thermocouple technique. Adapted from Shaw (2005).

Analysis of the thermoelectric circuit is fundamental to correctly understanding the relationship between the *EMFs* generated and the temperature, and to determine how the circuit junctions can influence the resulting *EMF* (Santos et al., 2013).

In a circuit composed of two different metallic materials (A and B) with their junctions at temperatures *T1* and *T2*, respectively, and with *T1* = *T2*, an *EMF* (*ER*) appears (see Figure 2), and its value is the sum of the voltages at thermojunctions 1 and 2 (Eq.1).

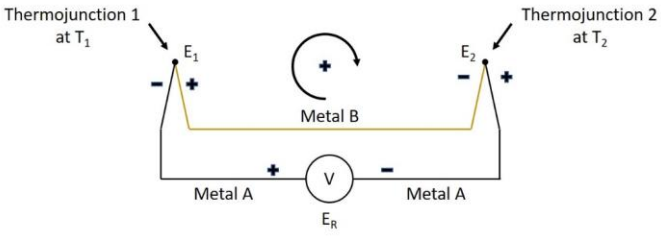

Figure 2. Basic thermoelectric circuit.

$$E_R = E_1 + E_2 \tag{1}$$

Voltages *E1* and *E2* are dependent on the temperature and the Seebeck coefficient (σ). This coefficient represents the voltage variation with the temperature, which is dependent on the nature of the thermocouple materials. In practice, this relation is generally constant, resulting in a linear function, as shown by Eq. 2.

$$E_R = \sigma_{AB} T_1 + \sigma_{BA} T_2 \tag{2}$$

where σ_{AB} and σ_{BA} represent the *Seebeck* coefficients at thermojunctions 1 and 2, respectively. It is important to note that $\sigma_{AB} = -\sigma_{BA} = \sigma$. Thus, Eq. 2 can be rewritten as follows (Eq. 3):

$$E_R = \sigma (T_1 - T_2) \tag{3}$$

From Eq. 3 it is possible to obtain one of the temperatures, for example, T_1, if the other (reference) temperature (in this case T_2) is known. Thus, Eq. 3 can be written for T_1 as follows (Eq. 4):

$$T_1 = T_2 + \frac{E_R}{\sigma}; \text{ if } \sigma \neq 0 \tag{4}$$

The value of E_R is obtained through a previous calibration of the system, in which each voltage value has a corresponding temperature. The calibration methods are also based on Eq. 3 and the aim is to correlate each temperature with a voltage value. The resulting graph obtained through this procedure is commonly called "the thermocouple calibration curve."

The same analysis previously described for a basic thermocouple circuit can be adopted for the workpiece-tool thermocouple method, as performed by Kaminise et al. (2014) aiming to study the influence of the toolholder material on the tool-chip interface temperature in turning. The method developed by Kaminise et al. (2014) to obtain the tool-chip interface temperature will be described in detail below, since it was the technique used in this investigation.

A schematic representation of a thermoelectric circuit in a tool-workpiece thermocouple system is shown in Figures 3(a) and 3(b).

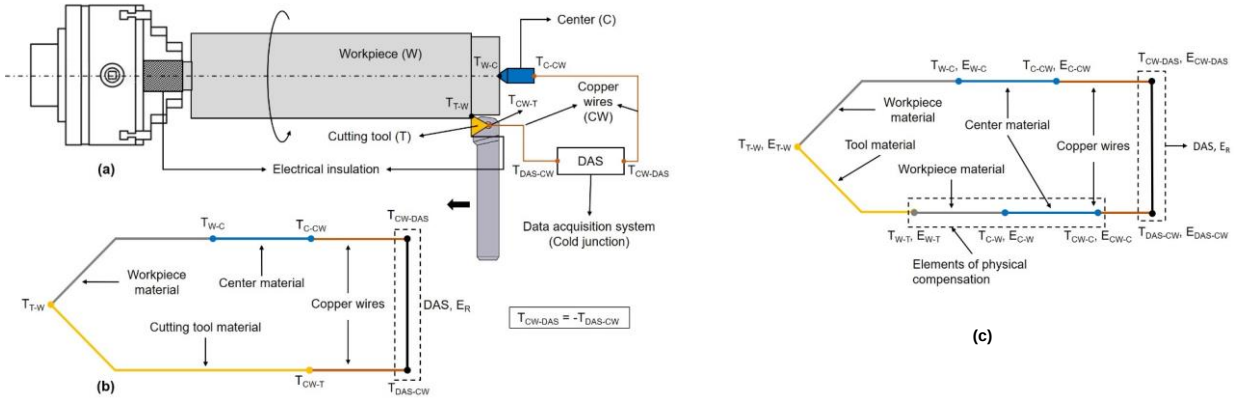

Figure 3. (a) Schematic representation of a thermoelectric circuit in a tool-workpiece thermocouple system and (b) circuit simplification showing its elements and thermojunctions. (c) Tool-workpiece thermoelectric circuit with physical compensation (Kaminise et al., 2014).

It can be noted that, besides the tool-workpiece contact, the circuit is composed of different materials connected by secondary junctions. On analyzing the voltage produced by each thermojunction in Figure 3(b), it is possible to obtain the resulting electromotive force, E_R, as previously described:

$$E_R = E_{T\text{-}W}(T_{T\text{-}W}) + E_{W\text{-}C}(T_{W\text{-}C}) + E_{C\text{-}CW}(T_{C\text{-}CW}) + E_{CW\text{-}DAS}(T_{CW\text{-}DAS}) + \ldots \tag{5}$$

$$\ldots + E_{DAS\text{-}CW}(T_{DAS\text{-}CW}) + E_{CW\text{-}T}(T_{CW\text{-}T})$$

As $E_{CW\text{-}DAS} = -E_{DAS\text{-}CW}$, Equation 5 is reduced to Equation 6:

$$E_R = E_{T\text{-}W}(T_{T\text{-}W}) + E_{W\text{-}C}(T_{W\text{-}C}) + E_{C\text{-}CW}(T_{C\text{-}CW}) + E_{CW\text{-}T}(T_{CW\text{-}T}) \tag{6}$$

The factors in Eq. 6 represent the voltages produced by each thermojunction. Each factor is dependent on the corresponding temperature and the resulting voltage varies according to the voltage produced at each thermojunction (Stephenson, 1993). Thus, when determining the temperature at $T_{T\text{-}W}$, it is important to consider the influence of the secondary thermojunctions on the E_R value. Kaminise et al. (2014) proposed an alternative to offset the voltages produced at the secondary thermojunctions. They added a couple of new elements to the circuit composed of workpiece and lathe center materials, as shown in Figure 3(c).

On applying the Kirchhoff law to the circuit of Figure 3(c), Equation 7 is obtained:

$$E_R = E_{T\text{-}W} + E_{W\text{-}C} + E_{C\text{-}CW} + E_{CW\text{-}DAS} + E_{DAS\text{-}CW} + E_{CW\text{-}C} + E_{C\text{-}W} + E_{W\text{-}T} \tag{7}$$

Considering that the temperatures of the furthermost junctions ($T_{W\text{-}C}$, $T_{C\text{-}CW}$, $T_{CW\text{-}DAS}$, $T_{DAS\text{-}CW}$, $T_{CW\text{-}C}$ and $T_{C\text{-}W}$) do not vary over time, and that they are at the same temperature (e.g., at room temperature), i.e., $T_{W\text{-}C} = T_{C\text{-}CW} = T_{CW\text{-}DAS} = T_{DAS\text{-}}$

$_{CW} = T_{CW-C} = T_{C-W}$ = constant, then $E_{W-C} = E_{C-CW} = E_{CW-DAS} = E_{DAS-CW} = E_{CW-C} = E_{C-W}$. As $E_{W-C} = -E_{C-W}$, $E_{CW-DAS} = -E_{DAS-CW}$ and $E_{CW-C} = -E_{C-CW}$, Eq. 7 is reduced, as shown in Eq. 8.

$$E_R = E_{T-W}(T_{T-W}) + E_{W-T}(T_{W-T}) \tag{8}$$

Since the junctions T-W and W-T are composed of the same materials, their *Seebeck* coefficients have the same value (σ). Thus, Eq. 8 can be rewritten for the temperature at the tool-chip interface $T_{int} = T_{T-W}$, as in Eq. 9.

$$T_{int} = T_{W-T} + \frac{E_R}{\sigma} \tag{9}$$

The tool-chip interface temperature, T_{int}, can therefore be obtained by means of the resultant voltage, E_R, the temperature at the cutting tool-compensation element junction, T_{W-T} and *the Seebeck* constant, σ.

It is important to mention that T_{W-T} can vary during the cutting process, mainly in the case of inserts, in which the junction *W-T* is close to the cutting zone. Thus, not only in the calibration step but also in the cutting step, it is necessary to monitor and register this temperature in order to include it to calculate T_{int}.

3. MATERIALS AND METHODS

The arrangement to calibrate the tool-workpiece thermocouple system was set up on the same conventional lathe (Romi II-520) used for the turning tests. The method developed by Kaminise at al. (2014) and mentioned in the introduction section was reproduced and used in this investigation.

Figure 4 show the main components of the arrangement for calibration at high temperatures. The same configuration was used to calibrate the system at sub-zero temperatures, but the torch was replaced with a copper delivery nozzle. It should be noted that Figure 4 represents a top view of the system, but with the modifier live center turned 90° counterclockwise to better show the internal parts.

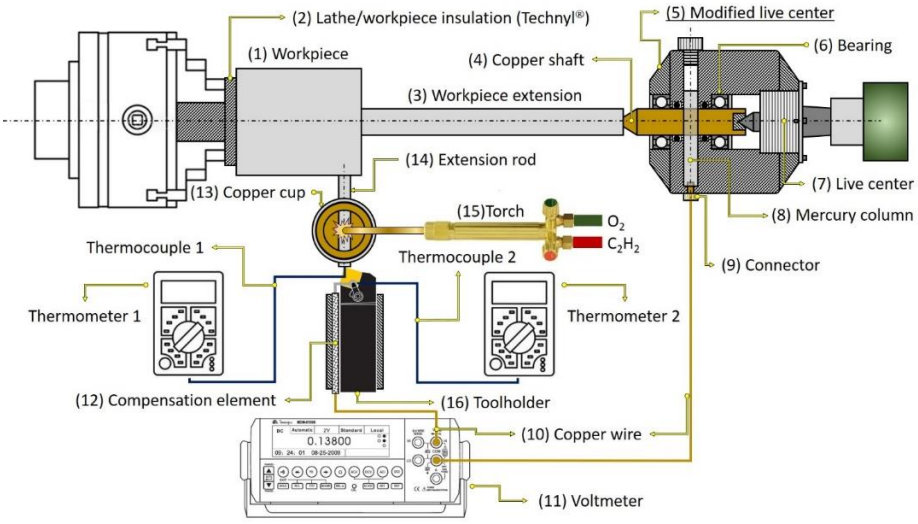

Figure 4. Arrangement of equipment used to calibrate the tool-workpiece thermocouple system.

The workpiece consisted of a quenched and tempered AISI D6 tool steel (57 HRC) cylindrical bar with a diameter of 109.8 mm and length of 133 mm (1). To prevent a temperature variation at the contact between the workpiece and the rotating cooper shaft (4) during the calibration and turning tests, these parts were kept distant from each other by means of a workpiece extension (∅ 25 mm x 200 mm) (3), which was welded to the workpiece. For the calibration procedure, an extension rod (∅ 10 mm x 95 mm) (14) of the same workpiece material was also fixed to the workpiece in order to accelerate the temperature change. A copper cup (13) insulated with glass wool was attached to the extension rod with the purpose of concentrating the heat supplied by the torch, or the mist of liquid nitrogen in the case of sub-zero calibration. A full form PCBN insert SNGN 120412S02520M 7925 manufactured by Sandvik Coromant was used as the cutting tool and it was clamped on a toolholder code DSBR 2525M 12.

It can also be observed in Figure 4 that a compensation element (12) is used to close the electrical circuit between the insert and the copper wire (10), which is connected to the voltmeter (11). The voltmeter measures the resultant electromotive force in the circuit. The compensation element was made of a thermoplastic tube filled with compacted chips of the workpiece material. The end, close to the insert, is composed of a small piece also made of the workpiece

material and attached to the insert by means of the toolholder clamp, together with the end of thermocouple 2 (K-type), which measures the temperature variation at this point during the calibration. Thermocouple 1 (K-type) measures the temperature variation at the contact point between the insert and the extension rod (14). In order to ensure the closing of the circuit, even though the workpiece is rotating, a modified live center was used (5). In this device there is a copper shaft (4) supported by two ball bearings (6). This shaft is in contact with the workpiece extension and rotates with it when the lathe is turned on, in the case of turning tests. The copper shaft then passes through a column of liquid mercury (8) that is also in contact with a copper connector (9) at the bottom of the modified live center, to which a copper wire (10) is connected, which passes to the second connection of the voltmeter, closing the electrical circuit of the system. It is important to highlight that all of these elements are isolated from the lathe using components manufactured of Technyl® (but another type of insulator could be used).

Figure 5 shows a representative electrical circuit for the tool-workpiece thermocouple system used in this investigation.

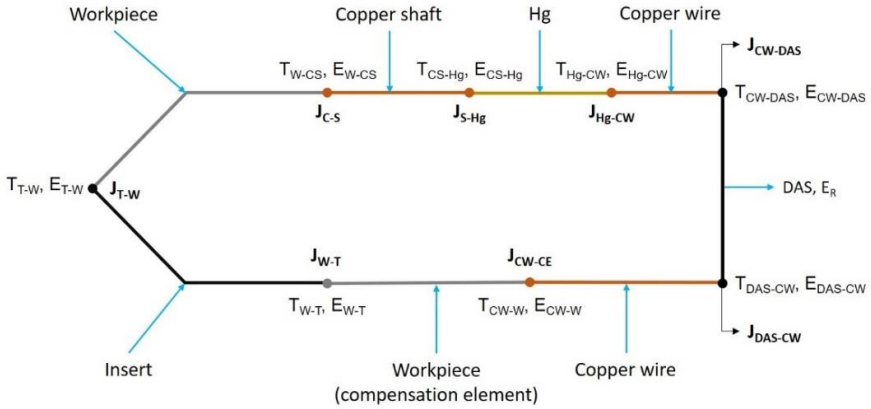

Figure 5. Electrical circuit for the tool-workpiece thermocouple system.

The circuit is basically composed of four different materials with eight thermoelectric junctions (e.g., **J_{W-T}** in Figure 5). Considering each junction as a source of FEM and using the Kirchhoff law, gives Eq. 10.

$$E_R = E_{T\text{-}W}(T_{T\text{-}W}) + E_{W\text{-}CS}(T_{W\text{-}CS}) + E_{CS\text{-}Hg}(T_{CS\text{-}Hg}) + E_{Hg\text{-}CW}(T_{Hg\text{-}CW}) + \cdots \quad (10)$$

$$\cdots + E_{CW\text{-}DAS}(T_{CW\text{-}DAS}) + E_{DAS\text{-}CW}(T_{DAS\text{-}CW}) + E_{CW\text{-}W}(T_{CW\text{-}W}) + E_{W\text{-}T}(T_{W\text{-}T})$$

In this investigation, it was assumed that $T_{W\text{-}CS} = T_{CS\text{-}Hg} = T_{Hg\text{-}CW} = T_{CW\text{-}DAS} = T_{DAS\text{-}CW} = T_{CW\text{-}W} = T_{room} = cte$.

From the principle that an inversion in the order of the elements that compose the circuit means a change in polarity of the FEM generated, e.g., $E_{CW\text{-}DAS} = -E_{DAS\text{-}CW}$, and because the copper shaft and the copper wire are of the same material and the compensation element is comprised of the same material as the workpiece, Eq. 10 can be rewritten as follows (Equations 11 and 12):

$$E_R = E_{T\text{-}W}(T_{T\text{-}W}) + E_{W\text{-}CS} + E_{CS\text{-}Hg} - E_{CS\text{-}Hg} + E_{CW\text{-}DAS} - E_{CW\text{-}DAS} - E_{W\text{-}CS} + E_{W\text{-}T}(T_{W\text{-}T}) \quad (11)$$

or $$E_R = E_{T\text{-}W}(T_{T\text{-}W}) + E_{W\text{-}T}(T_{W\text{-}T}) \quad (12)$$

As described in the introduction section, Eq. 12 can be rewritten as follows (Eq. 13):

$$E_R = \sigma_{T\text{-}W}.T_{T\text{-}W} + \sigma_{W\text{-}T}.T_{W\text{-}T} \quad (13)$$

where $\sigma_{T\text{-}W}$ and $\sigma_{W\text{-}T}$ are the Seebeck coefficients for the joints $J_{T\text{-}W}$ and $J_{W\text{-}T}$, respectively, which have the same value but opposite signs, i.e., $\sigma_{T\text{-}W} = -\sigma_{W\text{-}T}$. Thus, Eq. 13 becomes Eq. 14:

$$E_R = \sigma_{T\text{-}W}.T_{T\text{-}W} - \sigma_{T\text{-}W}.T_{W\text{-}T} \quad (14)$$

Finally, for $\sigma_{T\text{-}W} = K$, where "K" is the *Seebeck* coefficient for the tool-workpiece thermocouple, Eq. 14 can be rearranged for the tool-chip interface temperature as follows (Equations 15 and 16):

$$T_{T\text{-}W} = T_{W\text{-}T} + \frac{E_R}{K} \tag{15}$$

$$\text{or } K = \frac{E_R}{T_{T\text{-}W} - T_{W\text{-}T}} \tag{16}$$

Thus, during the calibration process it is necessary to monitor the temperatures at junctions ($J_{T\text{-}W}$ and $J_{W\text{-}T}$) and E_R at the same time, in order to obtain the value of K, which represents the slope of the straight-line $E_R \times (T_{T\text{-}W}\text{-}T_{W\text{-}T})$, in the case of linear behavior.

To calibrate the tool-workpiece thermocouple system at high temperatures, the tool-workpiece junction was heated using an oxyacetylene torch. It should be noted that the flame is directed to the extension rod, which is partially inside the copper cup. Thus, the temperature at the tool-workpiece junction is increased (by conduction).

The temperatures $T_{T\text{-}W}$ and $T_{W\text{-}T}$ were monitored using digital multimeters (Minipa ET-1400). The voltages generated by the tool-workpiece thermocouple circuit were measured with an Agilent 34405A multimeter. The data were registered by means of photos taken of the displays of these devices at a frequency of around 1 photo per second.

Although the tool-chip interface temperatures during machining will not assume sub-zero values, calibration was performed under this condition in order to check the correspondence between the experimental points obtained at low temperatures and those obtained at high temperatures, thereby improving the correlation index of the fitted curve. Thus, the calibration at sub-zero temperatures was performed using LN2 as the cooling fluid to refrigerate the extension rod and the tool-workpiece thermocouple, using a system developed by Leadebal et al. (2019b) and Fernandes et al. (2020). Liquid nitrogen was applied as a mist at 1.8 bar, 38 L/h and -196 ºC to calibrate the system.

Since the temperatures reach sub-zero values in this step, the instrument used to measure them was a thermometer Agilent 34970A, which is able to measure cryogenic temperatures with a resolution of 0.1 ºC. The multimeter used to measure the resultant voltage was the same as that used for high temperature calibration (Agilent 34405A). The values were recorded using the same procedure applied in the case of high temperature calibration.

After these two procedures, the two calibration curves $(T_{T\text{-}W} - T_{W\text{-}T}) \times ER$ were plotted on a single chart, which was used to obtain the calibration curve for the two-workpiece thermocouple system and then to obtain the chip-tool interface temperature.

The data acquisition system used for the calibration and to measure the tool-chip interface temperature was developed and constructed based on the Arduino Uno platform, with low-cost and open-source software and hardware. In order to monitor visually the temperatures in real time, the platform was integrated with Excel® by means of the app PLX-DAQ. Thus, the system was able to capture the analog signals generated by the tool-workpiece thermocouple system, promote a static gain, digitalize the signals for processing by the ATmega328 P microcontroller present in the Arduino board and display the results in Excel®.

To assemble the data acquisition system the following equipment was used:

- An Arduino UNO R3 board equipped with an ATmega328 P microcontroller to receive and process the analog signals from the thermocouples.
- An Avia Semiconductors HX711 module amplifier and A/D converter to amplify the analog signals coming from the thermocouples.
- A Maxim Integrated MAX31855 module to amplify and digitalize the analog signal coming from the K-type thermocouple welded on the compensation element.
- Arduino IDE 1.8.8 app to edit the codes for data acquisition.
- The Parallax Inc PLX-DAQ software program to integrate the Arduino platform and the Excel® app.

The temperature at the tool-chip interface is dependent on both the voltage (ER) generated in the tool-workpiece thermocouple system and the temperature measured by the K-type thermocouple at the compensation element. Since it was designed for K-type thermocouples, the integrated circuit MAX31855 was previously calibrated to provide temperature values according to the input voltage signals. In contrast, the integrated circuit HX711 is more appropriate for load cell applications, i.e., for mass/weight measurements. However, in this investigation, it amplified the voltage signal coming from the tool-workpiece thermocouple system and delivered it to the Arduino Uno board. The resulting voltage (ER) is applied in the calibration equation together with the temperature measured by the thermocouple placed at the end of the compensation element end, which is in contact with the PCBN insert, providing the tool-chip interface temperature.

In order to minimize the measurement error, the data acquisition system was calibrated. In this procedure, the acquisition module was connected to a laptop (Dell Inspiron 5558) with a 2.2 GHz processor and submitted to different voltages provided by an Agilent E3631A voltage supply. The voltage values supplied were then plotted against the values given by the acquisition system. Thus, it was possible to calculate the error of the acquisition system. The reference voltage ranged from 0 to 16 mV (17 values). To minimize the error, a correction factor present in the HX711 code was modified eight times in order to obtain the lowest value for the error. The correction factor that provided the lowest error was considered for the final tests.

The setup for temperature measurements was practically the same used to calibrate the system (see Figure 6) with some mandatory modifications, such as: (i) the extension rod was removed, (ii) the data acquisition system was connected

to the experimental setup, (iii) the K-type thermocouple was connected to the data acquisition system, (iv) the toolholder was placed upside down on the lathe turret in order to prevent chip accumulation and avoid an accident (liquid nitrogen directed towards the lathe operator). Thus, the LN2 delivery nozzle was placed from top to bottom towards the flank face of the insert, as shown in the detail of Figure 6.

The turning trials were carried out with a cylindrical bar of quenched and tempered AISI D6 tool steel with an initial diameter of 109.8 mm and average hardness of 57 HRC. The bar was divided into three sections each of ~24 mm. It can be noted that one of these sections was used for pre-tests in order to verify the behavior of the system when turning and adjusting it, if necessary, before the final tests. The other two sections were used to perform the final tests under dry and LN2 conditions. The sections were separated by circular grooves with 5 mm of depth, which enabled the depth of cut to be set.

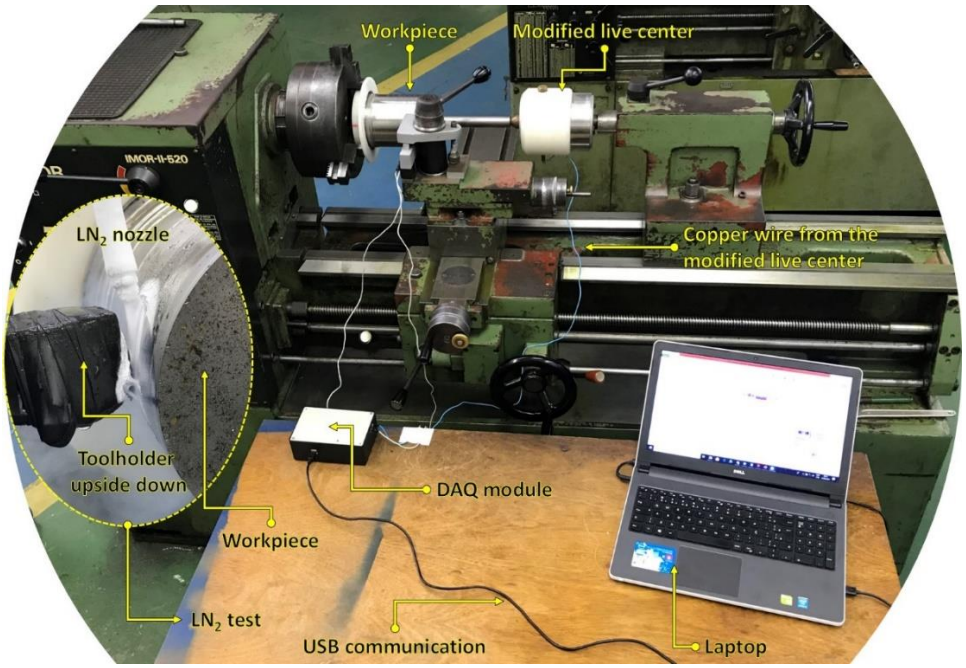

Figure 6. Setup for the tool-chip interface temperature measurement.

Three tests were performed for each condition (LN2 and dry) with different cutting speeds while keeping the feed rate (f = 0.1 mm/rev) and depth of cut (ap = 0.1 mm) constant. The same type of PCBN insert used in the calibration tests was applied in the turning tests. Table 1 summarizes the cutting conditions of the tests performed.

Table 1. Turning tests.

	Test	Cutting strategy	Cutting speed (m/min)
a_p = 0.1 mm f = 0.1 mm/rev	1	Dry	31
	2		48
	3		62
	5	LN2	31
	6		48
	7		62

At one of the ends of the compensation element a curved piece, also made of AISI D6 tool steel, was attached to facilitate its contact with the toolholder clamp.

Finally, LN2 was delivered on the flank face at a pressure of 1.8 bar and a flow rate of 38 L/h, using the system described by Leadebal Jr. et al. (2019a) and Leadebal Jr. et al. (2019b).

4. RESULTS AND DISCUSSION

In order to obtain the calibration curve for the tool-workpiece system, the experimental points for subzero and for high temperature calibrations were combined, giving the chart shown in Figure 7.

It can be noted that the experimental points for subzero and high temperatures fit the same linear curve (in red) almost perfectly, and this was used to represent the final calibration curve for the tool-workpiece thermocouple system proposed herein. The calibration equation is also shown on the chart.

Figure 8 shows the average tool-chip interface temperatures as a function of the cutting speed and cooling strategy. These average temperatures were obtained taking into account the values representing the steady-state conditions.

It can be noted that the average tool-chip interface temperature increases with the cutting speed for both cooling strategies. The tool-chip interface temperature increases with the cutting speed because additional energy is introduced into the process of chip formation, resulting in extra heat conversion and higher temperatures. High cutting temperatures can be noted even when low cutting speeds were applied.

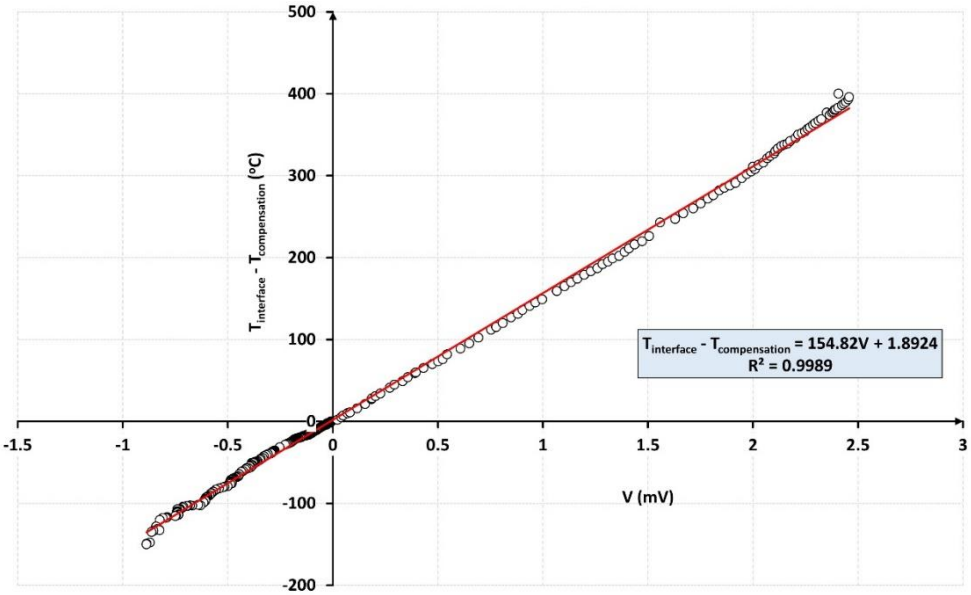

Figure 7. Final calibration curve.

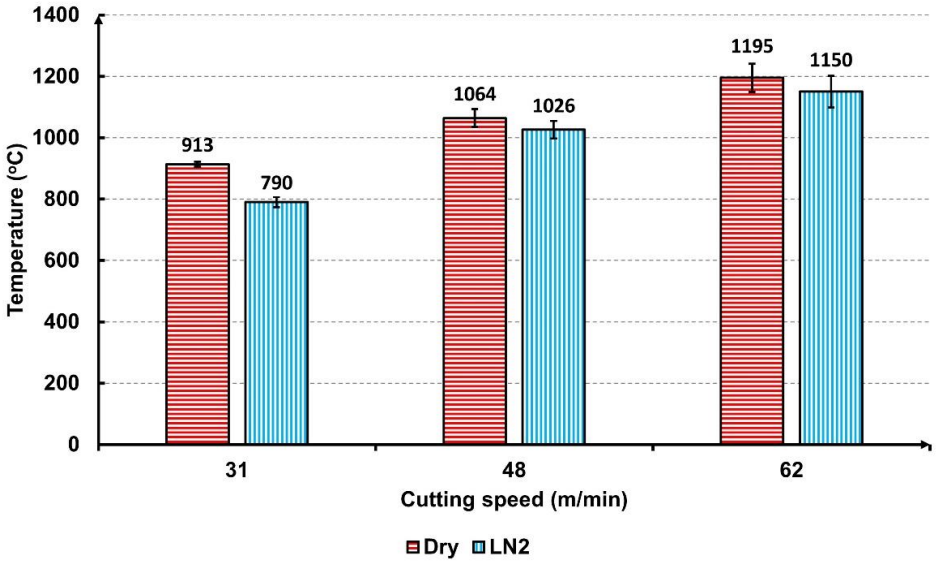

Figure 8. Tool-chip interface temperature as a function of cutting speed and cooling strategy.

It is noted that the LN2 strategy was in general able to reduce the average tool-chip interface temperature to some degree as compared to the dry cutting, although this reduction was not so expressive. In this case, the highest estimated value was of 123 °C for the lowest cutting speed (31 m/min). At higher cutting speeds the ability of the LN2 strategy to reduce the average tool-chip interface temperature was reduced. The difference between the temperatures under dry and LN2 conditions were of 38 and 45 °C at the cutting speeds of 48 and 62 m/min, respectively. It is important to remember

that in this investigation liquid nitrogen was delivered only at the flank face, with the LN2 flow direction opposite to the workpiece rotation (see Figure 22), and at an operating pressure (inside the LN2 container) of only 1.8 bar. Certainly, this set of conditions played an important role in the results of tool-chip interface temperature obtained.

As it is known, an important phenomenon that can affect the capacity of a cutting fluid to absorb heat from a heated surface (flank face, for example) is the Leidenfrost effect. In brief, this phenomenon is characterized by forming a low thermal conductivity vapor film, which covers the heated surface and prevents direct contact with the liquid, reducing the thermal convection coefficient and then the efficiency of the surface cooling process (Gonçalves et al., 2021). It is also known that the gas film thickness of the Leidenfrost phenomenon is inversely proportional to the liquid velocity (Gan et al., 2021). Thus, the lower the operating pressure, the lower would be the fluid velocity, promoting the Leidenfrost effect that impairs the heat transfer process from the cutting zone to the liquid nitrogen. In this investigation, because of the constructive limitations of our LN2 container, the operating pressure was kept at a relatively low value (1.8 bar). Regarding to this fact, it is still important to remember that the LN2 pressure drops along its way up to the delivery point. Thus, although it has not been measured in this investigation, the pressure at the outlet certainly was below the pressure inside the LN_2 container (operating pressure). Additionally, through Figure 22, it is noted that the direction of the workpiece rotation is opposite to the liquid nitrogen delivering, which may have contributed to reduce the heat transfer process. In this case, the toolholder was put upside down in order to prevent delivering liquid nitrogen towards the lathe operator's face, avoiding accident. At lower cutting speeds, as at 31 m/min, this effect is reduced, and the liquid nitrogen is most likely to be able to reduce the tool-chip interface temperature more effectively. The temperature oscillation under LN_2 condition can also be explained due to the set of conditions that promotes the instability of the boundary layer between the tool flank face and the liquid nitrogen. Thus, it is suggested that the technique proposed in this work is applied at different operating pressures (or delivery pressures) in order to investigate, among others, the influence of this variable in the chip-tool interface temperature.

5. CONCLUSIONS

In this study, the tool-chip interface temperature during the turning of quenched and tempered AISI D6 tool steel was investigated under dry conditions and with liquid nitrogen delivered at the flank face of PCBN inserts. An experimental system was specially developed, based on the tool-workpiece thermocouple technique. From the results obtained, the following conclusions can be drawn:

- The tool-workpiece thermocouple method is extremely laborious and difficult to perform but can be successfully used to measure the tool-chip interface temperature when turning hardened tool steels with the application of LN_2.
- The tool-chip interface temperature increases with the cutting speed, regardless of the cooling conditions.
- Liquid nitrogen was effective in reducing the tool-chip interface temperature (on average) when the cutting speed was of 31 m/min, but it was practically ineffective at the highest cutting speeds, probably due to the Leidenfrost phenomenon added to the counterflow effect of liquid nitrogen produced by the workpiece rotation. These same phenomena may also have provoked considerable oscillation in the tool-chip interface temperature under LN_2 condition.

6. ACKNOWLEDGEMENTS

The authors would like to thank to CAPES and CNPq.

7. REFERENCES

Dosbaeva G.K., El Hakim M.A., Shalaby M.A. et al., 2015. "Cutting temperature effect on PCBN and CVD coated carbide tools in hard turning of D2 tool steel". In *Int J Refract Met Hard Mater*, Vol. 50, pp. 1-8.

Sharma R., Bansal V., Nischal C., 2015. "Effect of cutting parameter on hard turning by using different lubricating conditions: A review". In *International Journal of Engineering Trends and Technology*, Vol. 30, No. 2, pp. 75-82.

Hashimoto F., Guo Y.B., Warren A.W., 2006. "Surface integrity difference between hard turned and ground surfaces and its impact on fatigue life". In *Ann CIRP*, Vol. 55, No. 1, pp. 81-84.

Benedicto E., Carou D., Rubio E.M., 2017. "Technical, economic and environmental review of the lubrication/cooling system used in machining processes". In *Procedia Eng*, Vol. 184, pp. 99-116.

Malek J., Desai T.N., 2019. "Prioritization of sustainable manufacturing barriers using Best Worst Method". In *J Cleaner Prod*, Vol. 226, pp. 589-600.

Del Re F., Dix M., Tagliaferri F., 2019. "Grinding burn on hardened steel: characterization of onset mechanisms by design of experiments". In *Int J Adv Manuf Technol*, Vol. 101, pp. 2889-2905.

Leadebal Jr. W.V., Melo A.C.A., Oliveira A.J. et al., 2019a. "Tool wear and chip analysis after the hard turning of AISI D6 steel assisted by LN2". In *Mach Sci and Technol*, Vol. 23, No. 6, pp. 886-905.

Leadebal Jr. W.V., Melo A.C.A., Oliveira A.J. et al., 2019b. "Effects of cryogenic cooling on the surface integrity in hard turning of AISI D6 steel". In *J Braz Soc Mech Sci Eng*; 40(1):1-14.

Shokrani A., Dhokia V., Muñoz-Escalona P. et al., 2013. “State-of-the-art cryogenic machining and processing”. In *Int J Computer Integr Manuf*; 26(7):616-648.

Biček M., Dumont F., Courbon C. et al., 2012. “Cryogenic machining as an alternative turning process of normalized and hardened AISI 52100 bearing steel”. In *J Mat Process Technol*; 212:2609-2618.

Hong S.Y., Ding Y., 2001. “Cooling approaches and cutting temperatures in cryogenic machining of Ti-6Al-4V”. In *Int J Mach Tools Manuf*; 41:1417-1437.

Dhar N.R., Paul S., Chattopadhyay A.B., 2002. “Role of cryogenic cooling on cutting temperature in turning steel”. In *Transactions of the ASME*; 124:146-154.

Kaminise A.K., Guimarães G., Da Silva M.B., 2014. “Development of a tool–work thermocouple calibration system with physical compensation to study the influence of tool-holder material on cutting temperature in machining”. In *Int J Adv Manuf Technol*; 73:735-747.

Shaw M.C. Metal Cutting Principles. 2nd ed. Oxford NY: Oxford University Press; 2005.

Santos Jr. M.C., Machado A.R., Barrozo M.A.S. et al., 2013. “Influence of Thermoelectric Junctions on the Electrical Signals Generated by the Tool-Workpiece Thermocouple System in Machining”. In *Measurement*; 46:2540-2546.

Stephenson D.A., 1993. “Tool-work thermocouple temperature measurements: Theory and Implementation Issues”. In *Transactions of the ASME*; 115(4):432-437.

Fernandes M.E.P., Melo A.C.A., Oliveira A.J. et al., 2020. “Hard turning of AISI D6 tool steel under dry, wet and cryogenic conditions: An economic investigation aimed at achieving a sustainable machining approach”. In *Cleaner Eng Technol*; 1:100022.

Gonçalves D.M., Sanchez L.E.A., Verdério Júnior, S.A., 2021. “Correlation between Leidenfrost temperature, cooling capacity and machining temperature: An experimental study of cutting fluids”. In *RETERM Thermal Engineering*; 20(3):10-15.

Gan Y., Wang Y., Liu K. et al., 2021. “The development and experimental research of a cryogenic internal cooling turning tool”. In *Journal of Cleaner Production*; 319:1-12.

8. RESPONSIBILITY NOTICE

The authors are the only responsible for the printed material included in this paper.